AECL-9111

ATOMIC ENERGY OF CANADA LIMITED

L'ÉNERGIE ATOMIQUE DU CANADA LIMITÉE

ACOUSTIC EMISSION FROM ZIRCONIUM ALLOYS DURING MECHANICAL AND FRACTURE TESTING

Application de l'émission acoustique des alliages de zirconium lors d'essais mécaniques et de fissuration

C.E. COLEMAN

Chalk River Nuclear Laboratories

Laboratoires nucléaires de Chalk River

Chalk River, Ontario

October 1986 octobre

ATOMIC ENERGY OF CANADA LIMITED

ACOUSTIC EMISSION FROM ZIRCONIUM ALLOYS DURING MECHANICAL AND FRACTURE TESTING

by

C.E. Coleman

Metallurgical Engineering Branch
Chalk River Nuclear Laboratories
Chalk River, Ontario K0J 1J0
1986 October

AECL-9111

APPLICATION DE L'ÉMISSION ACOUSTIQUE DES ALLIAGES DE ZIRCONIUM LORS D'ESSAIS MÉCANIQUES ET DE FISSURATION

par

C.E. Coleman

RÉSUMÉ

On examine l'application de l'émission acoustique lors d'essais mécaniques et de fissuration sur des alliages de zirconium. L'émission acoustique permet de suivre quantitativement, avec succès, la fissuration retardée, par l'hydrure. Elle est surtout utile lorsqu'une grande sensibilité est nécessaire. Elle semble encourageante pour la fissuration par fatigue, par déformation sous traction et par corrosion sous contrainte mais demande davantage de travail pour séparer les phémomènes, avant de pouvoir l'appliquer quantitativement.

Ce rapport est basé sur une étude sollicitée pour l'American Society of Non-Destructive Testing Handbook: Volume 5, Acoustic Emission Testing.

Génie métallurgique
Laboratoires Nucléaires de Chalk River
Chalk River, Ontario, Canada K0J 1J0
1986 octobre

AECL-9111

ATOMIC ENERGY OF CANADA LIMITED

ACOUSTIC EMISSION FROM ZIRCONIUM ALLOYS DURING MECHANICAL AND FRACTURE TESTING

by

C.E. Coleman

ABSTRACT

The application of acoustic emission during the mechanical and fracture testing of zirconium alloys is reviewed. Acoustic emission is successful in following delayed hydride cracking quantitatively. It is especially useful when great sensitivity is required. Application to fatigue, tensile deformation and stress corrosion cracking appears promising but requires more work to separate phenomena before it can be used quantitatively.

This report is based on an invited review for the American Society of Non-Destructive Testing Handbook: Volume 5, Acoustic Emission Testing.

Metallurgical Engineering Branch
Chalk River Nuclear Laboratories
Chalk River, Ontario K0J 1J0
1986 October

AECL-9111

ACOUSTIC EMISSION FROM ZIRCONIUM ALLOYS DURING MECHANICAL AND FRACTURE TESTING

by

C.E. Coleman

1. INTRODUCTION

Acoustic emission (AE) has been used for monitoring deformation and cracking in zirconium alloys for over ten years. Its non-destructive and remote sensing features make it ideal for many laboratory applications where electrical and surface measurements or optical observations are impossible or too insensitive. In this review, examples of the signals emitted by zirconium alloys during tensile and fatigue testing and various cracking processes are cited to show the range and sensitivity of the technique. The limitations of the results are discussed and further work is recommended.

2. ACOUSTIC EMISSION

When a discrete deformation or cracking event takes place in a mechanical test specimen, transient elastic stress waves are released. This is acoustic emission. The waves have a small amplitude but can be detected by a piezoelectric crystal, which oscillates in a damped sinusoid at its resonant frequency. The signal is amplified and processed electronically. The number of AE counts measured for each event is the number of times the signal exceeds a trigger voltage. AE may be expressed in many ways, for example, as number of events, total counts or rate of counts. The energy of the signal may be measured or it may be analyzed by its amplitude or frequency distribution or it may be converted into an audible signal. The AE transducer may be placed directly onto the specimen or may be attached to the specimen via a wave guide or to the specimen grips. Often the signal is gated between two frequencies (usually 0.1 to 0.3 MHz) to minimize external interference and the amplifiers have gain settings up to about 95 dB for the greatest sensitivity. Beyond 95 dB gain background and electronic noise may be detected.

3. ZIRCONIUM ALLOYS

The α-phase of zirconium has a hexagonal close packed structure and when fabricated into components, tends to be highly textured. As a result, strength properties and deformation are anisotropic. Zirconium has a great affinity for hydrogen and oxygen; brittle hydrides form at room temperature and the surfaces are never free from oxide. Zirconium alloys are also susceptible to stress corrosion cracking. Acoustic emission has been used to study the complex situations developed during mechanical and chemical interactions.

The two main alloys used in the nuclear industry are Zr-1.2 at% Sn (called Zircaloy) and Zr-2.5 at% Nb. The former is an α-alloy; it is used for fuel sheathing, pressure tubes, calandria tubes and other internal structures in the reactors. Zr-2.5 at% Nb is an α/β alloy that is used for pressure tubes in CANDU reactors.

4. PLASTIC DEFORMATION

The AE response from plastic deformation is studied to separate the mechanisms of deformation, to find how material variables affect AE and to provide a datum for fracture tests.

Acoustically, zirconium alloys behave similarly to other materials during tensile testing (1-5). If slip is the predominant deformation mechanism, the majority of the AE is generated around the yield stress, starting at the proportional limit, Figure 1. At larger strains and up to ductile fracture the material is silent. This behaviour has been interpreted in terms of Gilman's model (6) for the variation in density of mobile dislocations as a function of plastic strain. Twins produce large bursts of noise and in large grained material or when a specimen is pulled in a direction in which slip is difficult the acoustic activity can continue up to fracture, Figure 2. After unloading and reloading at small strains, no AE is detected until the previous elongation is reached. This is the 'Kaiser effect' which has been widely reported for other materials.

Neutron irradiation can reduce AE (5). In experiments at room temperature on pure zirconium, twinning was suppressed by irradiation to a fluence of 4×10^{23} n/m^2 at 470 K; the specimens deformed by dislocations clearing out the irradiation damage in channels. This latter process is very quiet. When the irradiation damage was removed by annealing at 1 020 K, the original tensile properties were recovered, twinning occurred and copious AE was observed.

The acoustic emission signal associated with twin formation has been studied in more detail at room temperature using hardness impressions in large grained pure zirconium (7). The emission event took about 1 msec to complete but it consisted of about 1 000 separate pulses. These pulses were interpreted as being caused by single or groups of twinning dislocations being accommodated by the undeformed zirconium crystal lattice.

5. FATIGUE

To investigate the feasibility of on-line monitoring of fatigue, AE produced by the fracture and fatigue of heat-treated Zr-2.5 at% Nb has been studied at room temperature (4). For double and single edge notch specimens the total AE count was plotted as a function of the square root of the notch-edge opening displacement, D, which is proportional to K_I. The curves exhibited several stages, Figure 3, that were interpreted in

terms of the development of plastic zones. When the plastic zone was small, the slope of the AE-$D^{1/2}$ curve was usually greater than in later stages, when general yield was approached. Two fatigue tests, using simulated pressure cycling on tubes containing through-wall axial cracks, showed promise for continuous monitoring of cracks. The increment AE energy per cycle, dE/dN, increased with the fatigue crack growth rate, da/dN, as a power law, Figure 4. No crack closure AE was detected. In the presence of water the cracks provided signals that were up to 16 times more energetic, suggesting that fatigue would be easier to detect in the presence of liquids.

6. CRACKING OF SURFACE OXIDE

Tensile specimens of Zircaloy coated in a thin oxide, approximately 1 to 3 μm thick, behave acoustically like unoxidized specimens at room temperature, except for occasional energetic pulses at specimen deformations of 1 to 2% (3). These results were surprising because the oxide was expected to be brittle, although other oxide cracking may have been lost in the early stages of deformation.

The expected copious AE from oxide cracking has been confirmed from ring tensile tests at room temperature on Zircaloy fuel sheathing coated on the outside surface with thick oxides, up to 8 μm thick, produced by holding in steam at 1 270 K for times between 30 and 120 s (8). A typical result, Figure 5, consisted of two maxima in count rate, one at between 0.6 and 0.7 of the maximum load and the other at the maximum load. The mean and range of the maximum count rate for each peak, Table 1, were scattered, but

TABLE 1

Maximum count rate at each peak during ring tensile tests on Zircaloy fuel sheathing as a function of time at 1270 K. (Counting time: 30 s)

Time at 1270 K (s)	Peak 1 (count rate, per 30 s)		Peak 2 (count rate, per 30 s)	
	Mean	Range	Mean	Range
30	6 700	4 100 to 9 800	2 700	1 300 to 5 100
60	5 800	1 300 to 9 200	20 500	9 500 to 30 300
120	8 500		42 300	
120 (vacuum)			2 200	1 900 to 2 600

suggested that the rate at the first peak was independent of oxidation time while the rate at the second peak increased dramatically with oxidation time. Specimens with a very thin oxide (heated to 1 270 K in a vacuum for 120 s) had a peak in count rate at maximum load but the total number of counts and count rate were much smaller than with the oxidized specimens. Specimens oxidized for 60 s were loaded to points A to D, Figure 5, and examined by metallography and scanning electron microscope. At A, cracks with a spacing of about 30 μm were observed through the oxide and sub-surface layer. At B, the spacing of the cracks was reduced to about 15 μm, but at C there was a little further cracking, spacing of 11 μm, but now the oxide was spalling off. Much spallation was observed at D. AE from cracking in the oxide and oxygen-rich sub-surface layer was not distinguished.

7. STRESS CORROSION CRACKING

The first attempts to distinguish by AE the stages in cracking processes were only partially successful (1,9). Cox loaded double cantilever beam and fuel cladding tube specimens of Zircaloy in four environments - methanol-1% iodine solution, methanol-1% hydrochloric acid solution, 5% aqueous sodium chloride solutions at room temperature and fused nitrate-iodide salt mixture at 570 K - and recorded AE continuously, e.g. Figure 6. Metallography was performed at stages during some tests and after cracking the fracture surfaces were examined to correlate the cracking mechanism with the acoustic emissions.

Two characteristic acoustic signals were obtained; a continuous 'swishing' noise and a discontinuous 'cracking' noise (here 'swishing' and 'cracking' refer to the audio output). The fracture surfaces consisted of smooth cleavage facets separated by striations caused by ductile tearing and extensive slip and void formation. In the tests at 570 K on fuel sheathing, grain boundary separation was observed. Often the fracture surfaces were etched by the solutions.

Often an incubation period was observed before AE was detected. Swishing signals were associated with material dissolution and slip and the emission of gas bubbles - hydrogen if the specimen was cathodically polarized and oxygen when it was anodically polarized - as well as crack propagation. Discontinuous signals also indicated cracking but were also produced by extra twinning or cracking of the protective oxide. Thus, although several sources of noise were identified, no unique explanation of the signals was possible.

In iodine stress corrosion cracking of Zircaloy fuel sheathing the study of the crack initiation phase is difficult because crack initiation is spasmodic and crack propagation is too fast to be stopped at a relatively infrequent visual inspection. What is required is a rapid response indicator of cracking so that the load may be lowered before the crack

extends too far. An attempt has been made to use AE as the trigger (10) but it was not possible to stop crack growth while the cracks were less than 100 μm long (about 25% through the tube wall). Sometimes AE signals came from the apparatus during heating while the stress corrosion itself produced signals whose amplitude varied widely.

The application of AE to monitor stress corrosion cracking reliably requires fu~ther work.

8. DELAYED HYDRIDE CRACKING

The most successful application of AE to zirconium alloys has been with delayed hydride cracking (DHC) (11-21). This cracking has been responsible for failures of vessels in both the nuclear and chemical industries. The mechanism requires hydrogen to diffuse up a stress gradient and accumulate at a stress concentration where hydrides precipitate. If the stress is large enough, the hydrides crack. This sequence is then repeated and the crack grows in steps. The inference from this description is that there should be an incubation time before cracking starts and then the crack should grow in discrete jumps. This was confirmed by AE measurements. Subsequent work established the relationship between the acoustic signals and DHC; AE was then applied as a standard technique to study the important parameters of cracking.

In the first experiment using AE (11) a notched tensile specimen of Zr-2.5 at% Nb containing 0.9 at% hydrogen was loaded to 15.3 MPa$\sqrt{m}$ at 420 K and allowed to crack. Elongation, representing crack opening, and resistivity change across the notch, as well as AE counts, were measured simultaneously as a function of time, Figure 7. All three measurements showed the incubation time and changes that were associated with cracking and final failure.

The second experiment (12), on a cantilever beam specimen of Zr-2.5 at% Nb incorporated all the features exploited in later tests. The temperature and loading history were complicated, Figure 8, but the AE was clearly detected and measured.

After cooling from 570 K to 420 K the first AE was observed after 250 h, stage 1 of Figure 8. Thereafter it was intermittent but the times between each acoustic burst were at least 100 times less than the crack initiation time. When the temperature was raised to 520 K, AE stopped, stage 2, but it started again when the temperature was lowered back to 420 K, stage 3. On raising the temperature to 520 K, a few acoustic counts were detected in loop, stage 4, but these were thought to be spurious. Repetition of the thermal cycling about 520 K, stages 5 to 8, showed that if the specimen was cooled to 520 K it would emit noise, Figure 8. The effect of direction of temperature change was repeatable up to 550 K; when the temperature was raised to 550 K no AE was detected, stage 7, whereas when the specimen was cooled from 570 K to 550 K AE occurred, stage 10. Although AE occurred

above 520 K, it could be stopped by first lowering the temperature, stages 11 and 12, then heating back up to 520 K, stage 13.

Reducing the stress resulted in incubation periods. In stage 14 the temperature was lowered to 420 K and the nominal stress lowered to 550 MPa. No AE was detected within 3 h. When the stress was returned to 830 MPa, AE only started after an incubation period of 3 h, stage 15. AE stopped on reducing the stress to 690 MPa but started again after 17 h, stage 16. Stage 17 shows that the incubation period was longer than 40 h when the stress was lowered to 550 MPa. However, when the stress was raised back to 690 MPa, AE started immediately, stage 18. The ability to stop AE by raising the temperature to 520 K, stage 19, and re-start it by lowering the temperature to 520 K, stage 24, was confirmed. After a new incubation period of 4.5 h, induced by lowering the stress to 620 MPa, the specimen failed, stage 25.

The fracture surface associated with delayed hydrogen crack growth showed several coloured bands corresponding to oxidation at the higher temperatures. These could be directly related to the various stages of crack growth as indicated by acoustic emission.

In a third series of experiments (18), cantilever beam specimens of Zr-2.5 at% Nb were quenched at times less than and greater than the incubation time and examined metallographically. When the time was less than the incubation time, uncracked hydrides were observed at crack tips but when the time was greater than the incubation time, the hydrides were cracked.

All the above observations are the basis for accepting AE as a potent method for detecting DHC. Proportional correlations between AE counts and area of cracking have been established (15,17,19,21) and can be used to estimate crack lengths and velocities. The constant of proportionality appears to be independent of K_I and temperature although it varies slightly with each test. Thus, the usual practice is to break open the specimen after the test to confirm the constant. However, the constant varies with test apparatus, position of transducer and instrument settings. For example, Arora and Tangri (15) report a value of 2.4×10^3 counts/mm^2 while Coleman (17) obtained 5×10^5 counts/mm^2. Area of cracking is used because often the crack fronts are curved with the crack being longer in the midsection of the specimen. When translated into sensitivity, crack extensions of a few micrometres can be discerned thus many tests can be done on a single specimen. This leads to great efficiency in testing. Four examples are:

1. The determination of the threshold K_I, K_{IH}, for DHC by gradually reducing the load until AE (cracking) stops, Figure 9 (12). This method can be repeated several times on one specimen and is less time consuming than testing many specimens over a range of K_I values. Sagat et al. (21) have extended this idea and incorporated the correlation between AE and amount of cracking to control the loading

of the specimen by feedback of the AE signal through a computer. As well as gradually lowering K_I to obtain K_{IH}, the load can be adjusted to maintain a constant K_I in a cantilever beam specimen.

2. The determination of the effective solvus temperature, Ts, for hydrogen in zirconium by finding the temperature above which cracking ceases (13,18). The incubation time was determined about the expected value of Ts - below Ts the incubation time was short while above Ts no AE was observed for very long times, Figure 10.

3. The temperature dependence of crack velocity was determined for several metallurgical conditions using single specimens. Crack velocities were determined by allowing the crack to grow for short periods at one temperature then unloading, changing the temperature and reloading, Figure 11 (19).

4. Delayed hydride cracking in hydrogen gas is very rapid at room temperature but is sensitive to contamination (20). Small amounts of oxygen can slow or suppress cracking. Slow cracking was detected by AE after 0.1 volume % oxygen was added to the hydrogen atmosphere but could not be observed visually through a microscope, Figure 12.

AE has been used in attempts to establish the conditions for hydride cracking (22,23). Tensile specimens of Zr-2.5 at% Nb containing hydride platelets with normals parallel with the stressing direction produced AE at lower stresses and in larger quantities than specimens with hydrides with normals perpendicular to the stressing direction. Notched specimens produced more AE than smooth specimens. In both studies cracking associated with the hydrides was shown to be responsible for the AE, but the determination of the critical conditions for hydride cracking, which include stress, plastic strain and stress state (23,24), requires further work.

9. DISCUSSION

This survey has highlighted both the strengths and weaknesses of AE for monitoring the consequences of stressing zirconium alloys.

The technique is very sensitive. It can detect very small amounts of deformation and crack growth when only one mechanism is operating. This is especially useful close to thresholds of behaviour, for example, determining K_{IH}. In situations where more than one mechanism is involved, separation may be achieved by amplitude or frequency analysis (25). This technique has not been usefully applied to zirconium alloys. Care has to be taken if the signals are to be used to go beyond the question "Has the specimen cracked or deformed?" The original stress waves are modulated and attenuated as they travel through the specimen from their point of emission, so characterizing the initial event is difficult.

The transducers and supporting electronics are very stable. In one experiment (17), the detectors operated satisfactorily for 90 days with no adjustment. This kind of service is only possible when electrical and mechanical interference is minimized. Typically, furnace controls and switches, random line noise and radio signals have to be avoided. Testing at large loads on hydraulic tensile machines is currently impossible because of interference. Vacuum systems, boiling liquids (e.g., liquid nitrogen (3)) gas bubbling as the result of chemical reactions (1) and the release of pressurized gases can each contribute unwanted signals although the latter is sometimes used deliberately to check that the transducer is working.

10. CONCLUSIONS

The use of acoustic emission in the mechanical and fracture testing of zirconium alloys has been reviewed. Although AE has proved to be most useful in following delayed hydride cracking, its success in other applications is more modest and requires further work to separate the various operating deformation and cracking mechanisms and interfering signals.

11. REFERENCES

1. B. Cox, Corrosion, 30, (1974), 191-202.

2. V.N. Glygalo, V.V. Kirsanov, L.S. Kravtsova and A.G. Leshchinskii, Defektoskopiya, 3, (1975), 140-142.

3. B. Cox and C.E. Coleman, 'Acoustic Emission during the Tensile Testing of Zirconium Alloys', Atomic Energy of Canada Report, AECL-5831, May 1977.

4. E.B. Schwenk, P.H. Hutton and M. Igarashi, ASTM STP 633, (1977), 573-588.

5. M. Tokiwai, H. Kimura, H. Nakasa and H. Takaku, Proc. 4th Acoustic Emission Symposium, Tokyo, (1978), 2-62 - 2-88.

6. J.J. Gilman, J. App. Phys., 36, (1965), 2722.

7. V.S. Boiko, L.G. Ivanchenko and L.F. Krivenko, Sov. Phys. Solid State, 26, (1984), 1340-1.

8. C.E. Coleman, unpublished data.

9. B. Cox, Corrosion, 29, (1973), 157-166.

10. R. Haddad and B. Cox, 'Investigations of Crack Initiation during Environmentally Induced Cracking of the Zircaloys', Atomic Energy of Canada Report, AECL-8104, 1983 October.

11. C.E. Coleman and J.F.R. Ambler, ASTM STP 633, (1977), 589-607.

12. J.F.R. Ambler and C.E. Coleman, 2nd International Congress on Hydrogen in Metals, Paris, (1977), paper 3C10.

13. C.E. Coleman and J.F.R. Ambler, Can. Met. Quart., 17, (1978), 81-84.

14. A. Arora and K. Tangri, Int. J. Fracture, 15, (1979), R93-R95.

15. A. Arora and K. Tangri, Experimental Mechanics, 21, (1981), 261-267.

16. K. Tangri and X.Q. Yuan, 'Fracture Problems and Solutions in the Energy Industry', Pergamon Press, (1982), 27-38.

17. C.E. Coleman, ASTM STP 754, (1982), 393-411.

18. C.E. Coleman and J.F.R. Ambler, Scripta Met., 17, (1983), 77-82.

19. J.F.R. Ambler, ASTM STP 824, (1984), 653-674.

20. C.E. Coleman and B. Cox, ASTM STP 824, (1984), 675-690.

21. S. Sagat, J.F.R. Ambler and C.E. Coleman, "Application of Acoustic Emission to Hydride Cracking", Atomic Energy of Canada Report, AECL-9258, 1986 July.

22. C.J. Simpson, O.A. Kupcis and D.V. Leemans, ASTM STP 633, 1977, 630-642.

23. L.A. Simpson, Met. Trans., 12A, (1981), 2113-2124.

24. C.E. Coleman and D. Hardie, J. Less-Common Metals, 11, (1966) 168-185.

25. T.C. Lindley and P. McIntyre, 'Measurement of Crack Length and Shape during Fracture and Fatigue', Ed. C.J. Beevers, Engineering Materials Advisory Services, Ltd., 1980 pp. 285-344.

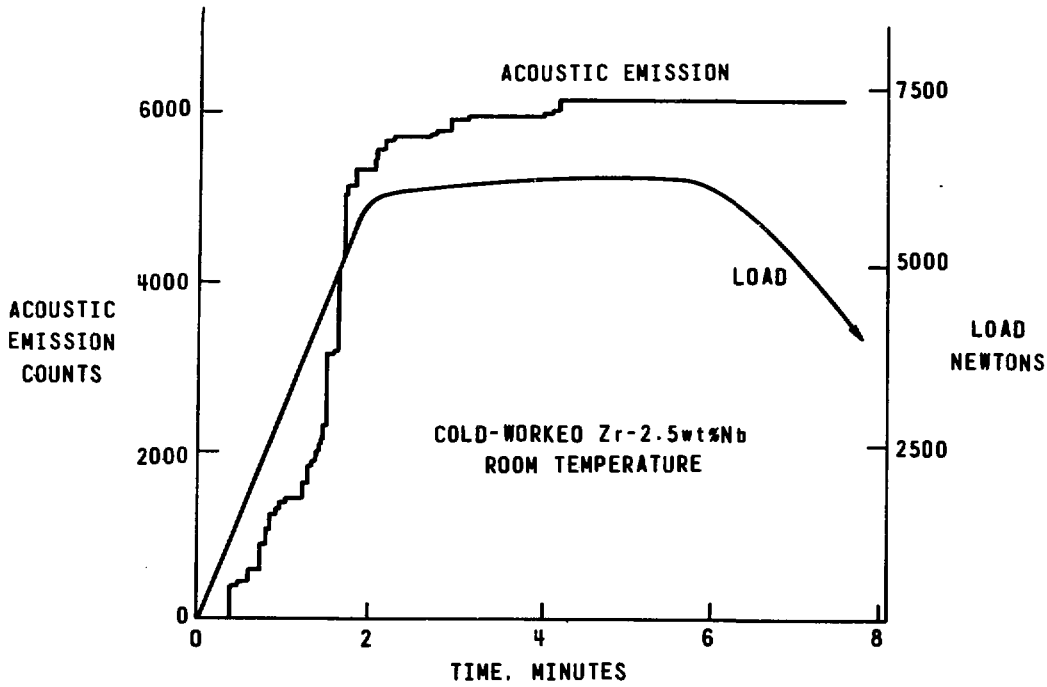

Figure 1: Acoustic emission during tensile testing of cold-worked Zr-2.5 at% Nb.

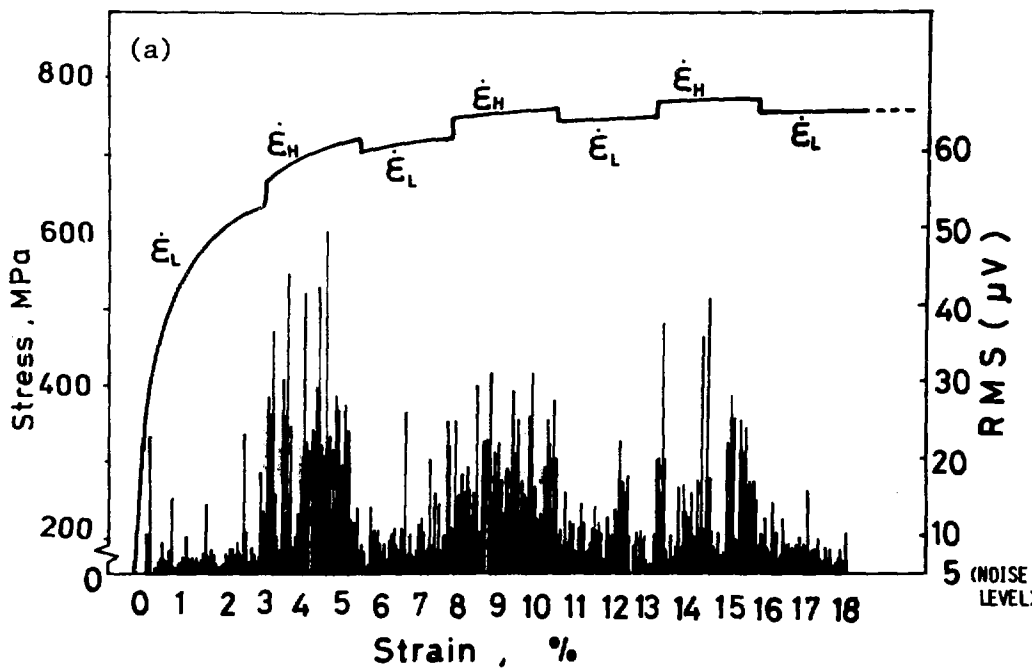

Figure 2: Continuous acoustic emission from twinning throughout tensile test on annealed pure zirconium at room temperature. $\dot{\varepsilon}_H = 6.6 \times 10^{-4}\ s^{-1}$, $\dot{\varepsilon}_L = 2.2 \times 10^{-4}\ s^{-1}$.

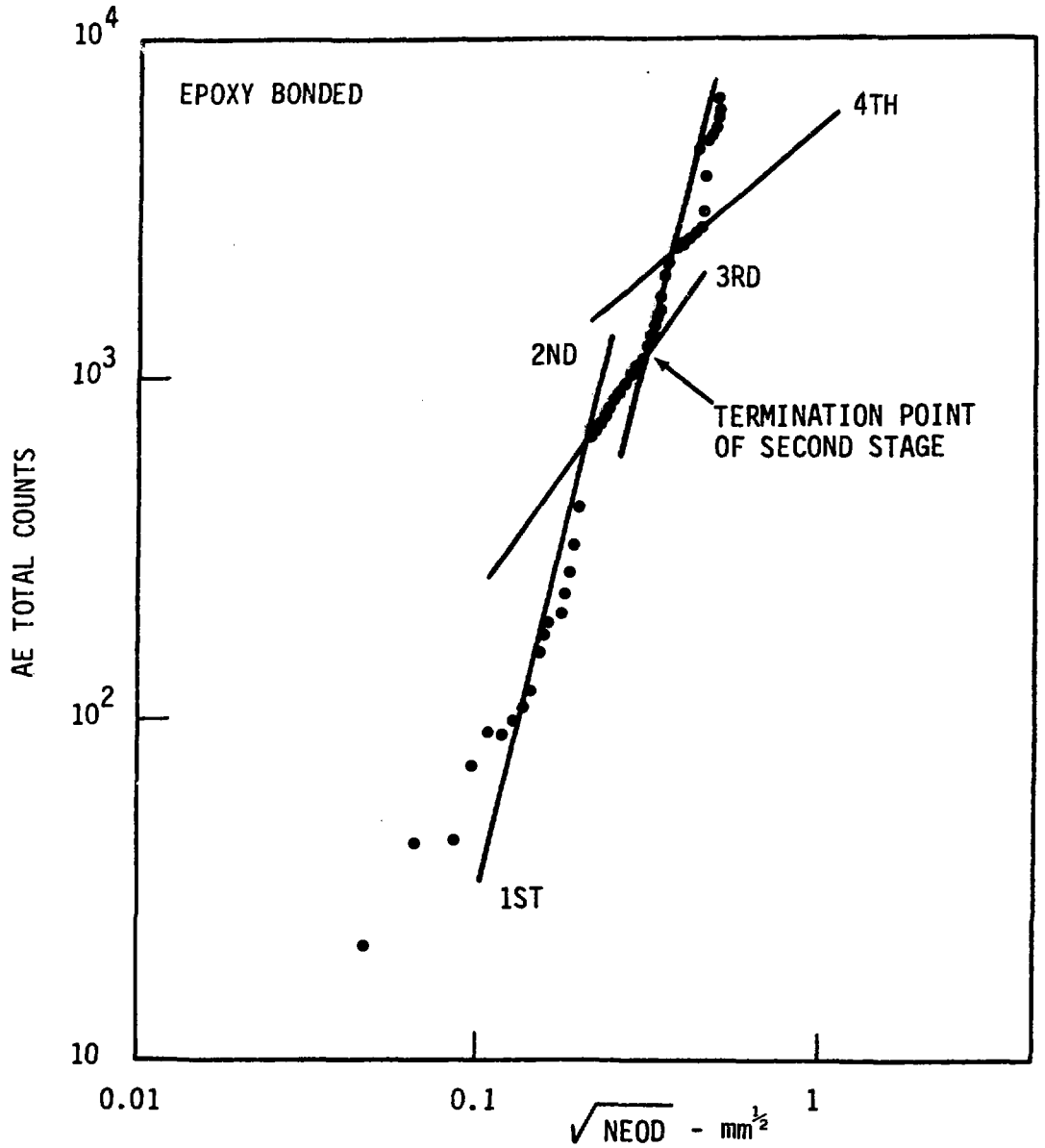

Figure 3: Cumulative acoustic emission counts as a function of notch-edge opening displacement (D in text) during room temperature fatigue testing of Zr-2.5 at% Nb.

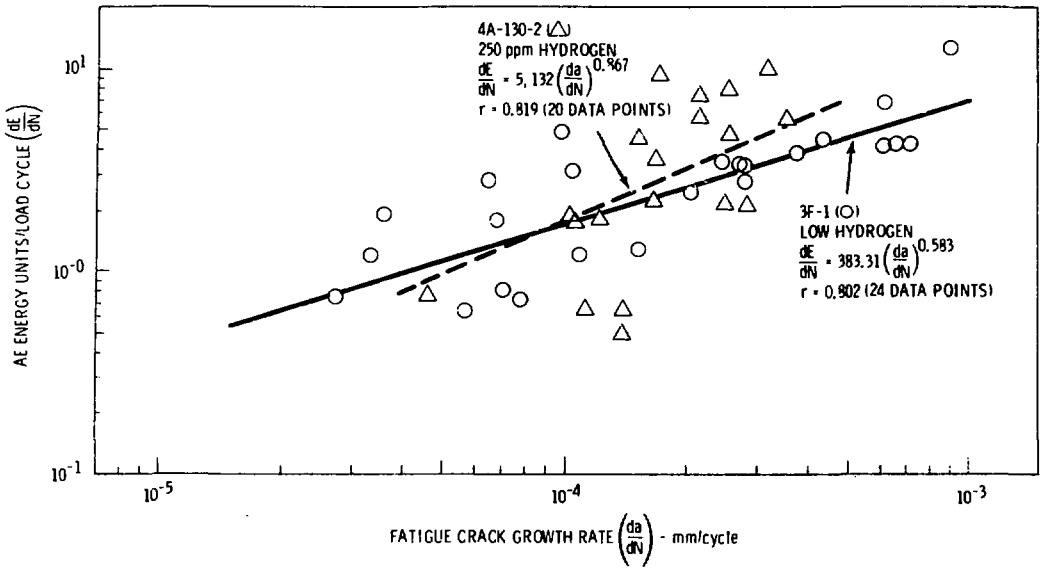

Figure 4: Acoustic emission energy per load cycle, dE/dN, as a function of fatigue crack growth rate, da/dN, for Zr-2.5 at% Nb tested at room temperature.

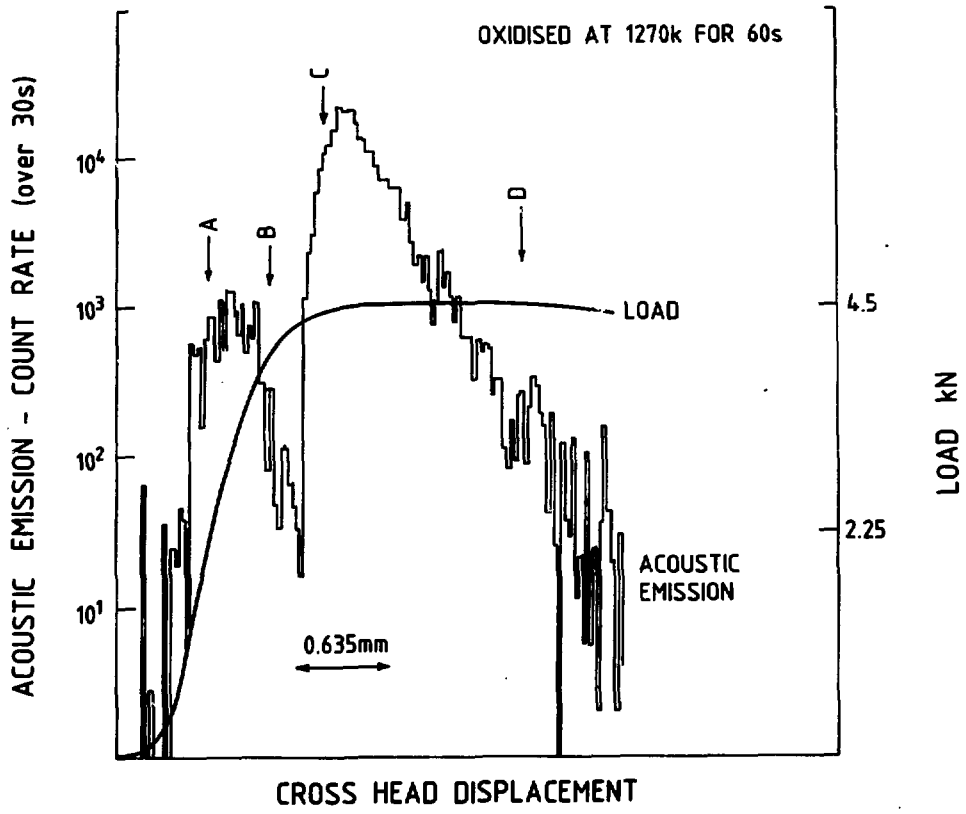

Figure 5: Acoustic emission during tensile testing at room temperature of pre-oxidized rings of Zircaloy fuel sheathing.

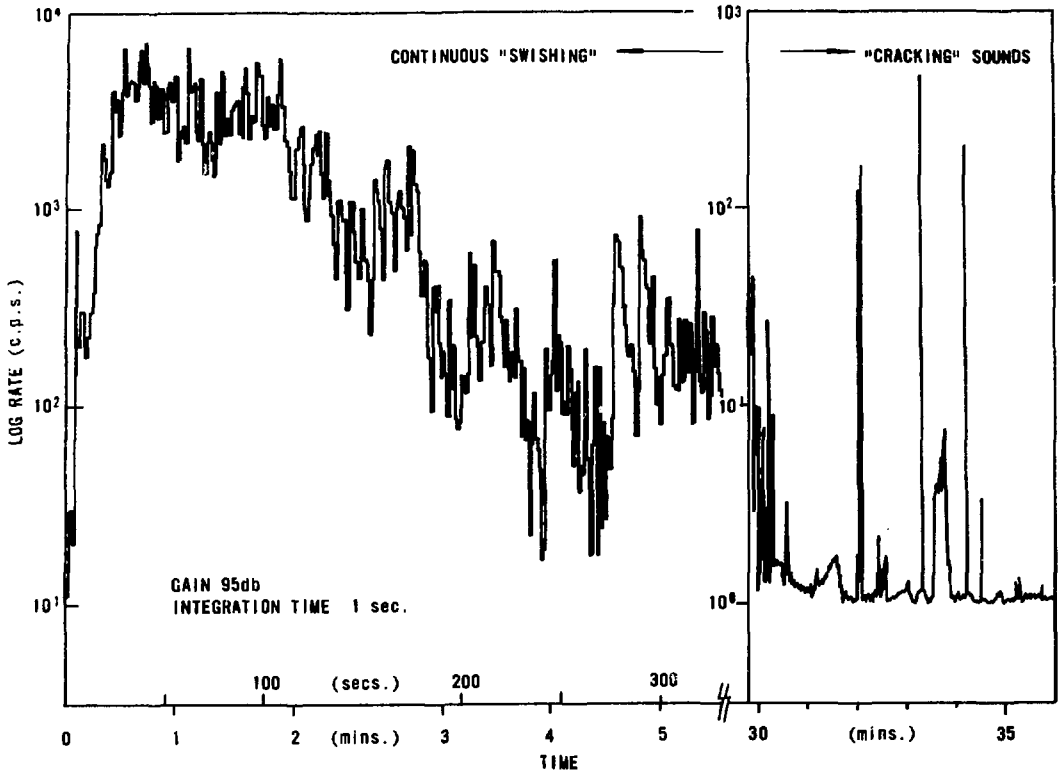

Figure 6: Acoustic emission versus time traces for a double cantilever beam specimen of Zircaloy loaded at room temperature in methanol-HCL solution.

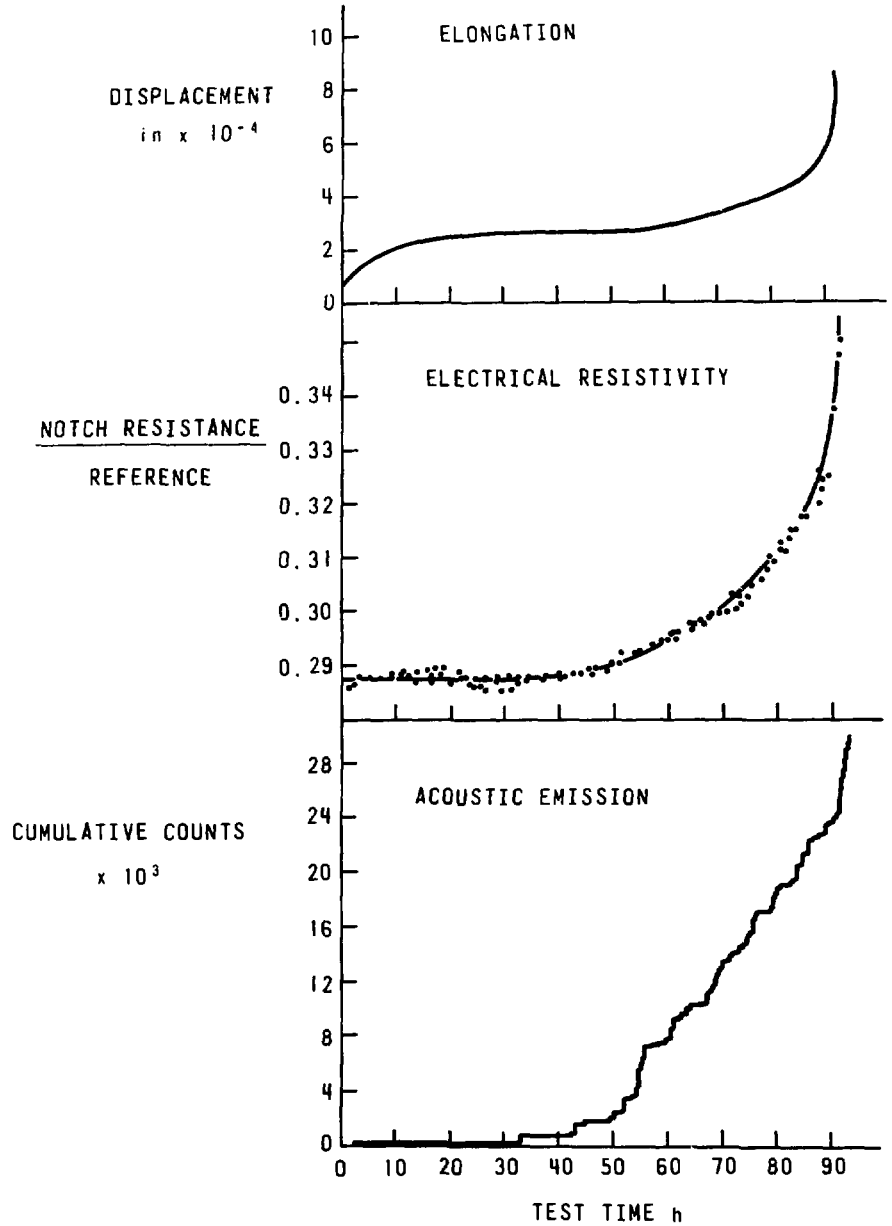

Figure 7: Comparison of resistivity change, displacement change and acoustic emission during delayed hydride cracking test on round notched bar of Zr-2.5 at% Nb containing 0.9 at% hydrogen at 420 K and 15.3 MPa$\sqrt{m}$.

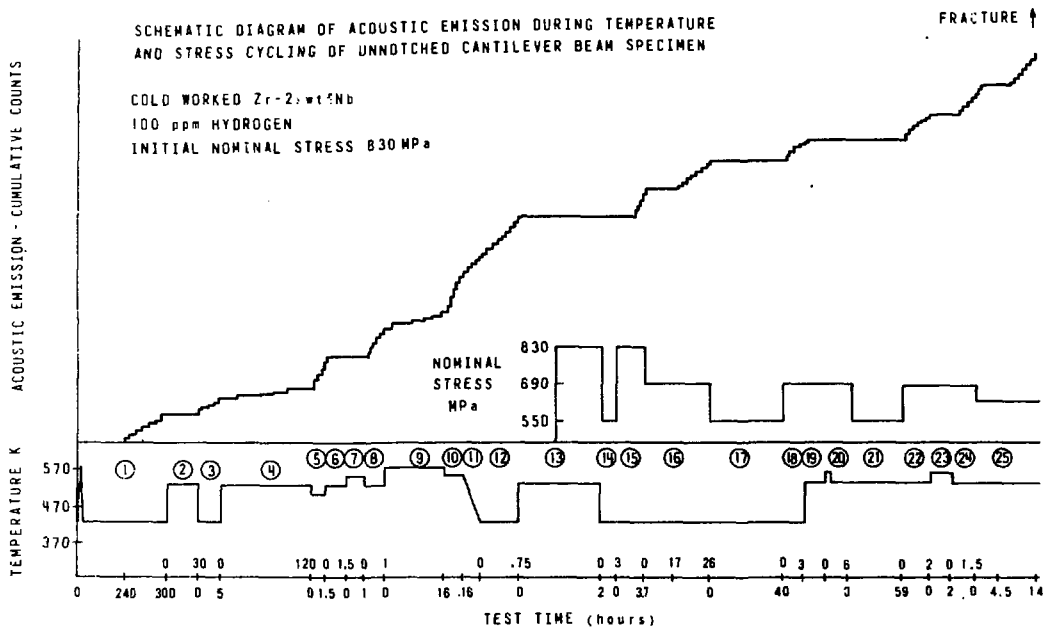

Figure 8: Schematic diagram of acoustic emission during temperature and stress cycling of unnotched cantilever beam specimen of Zr-2.5 at% Nb containing 0.9 at% hydrogen.

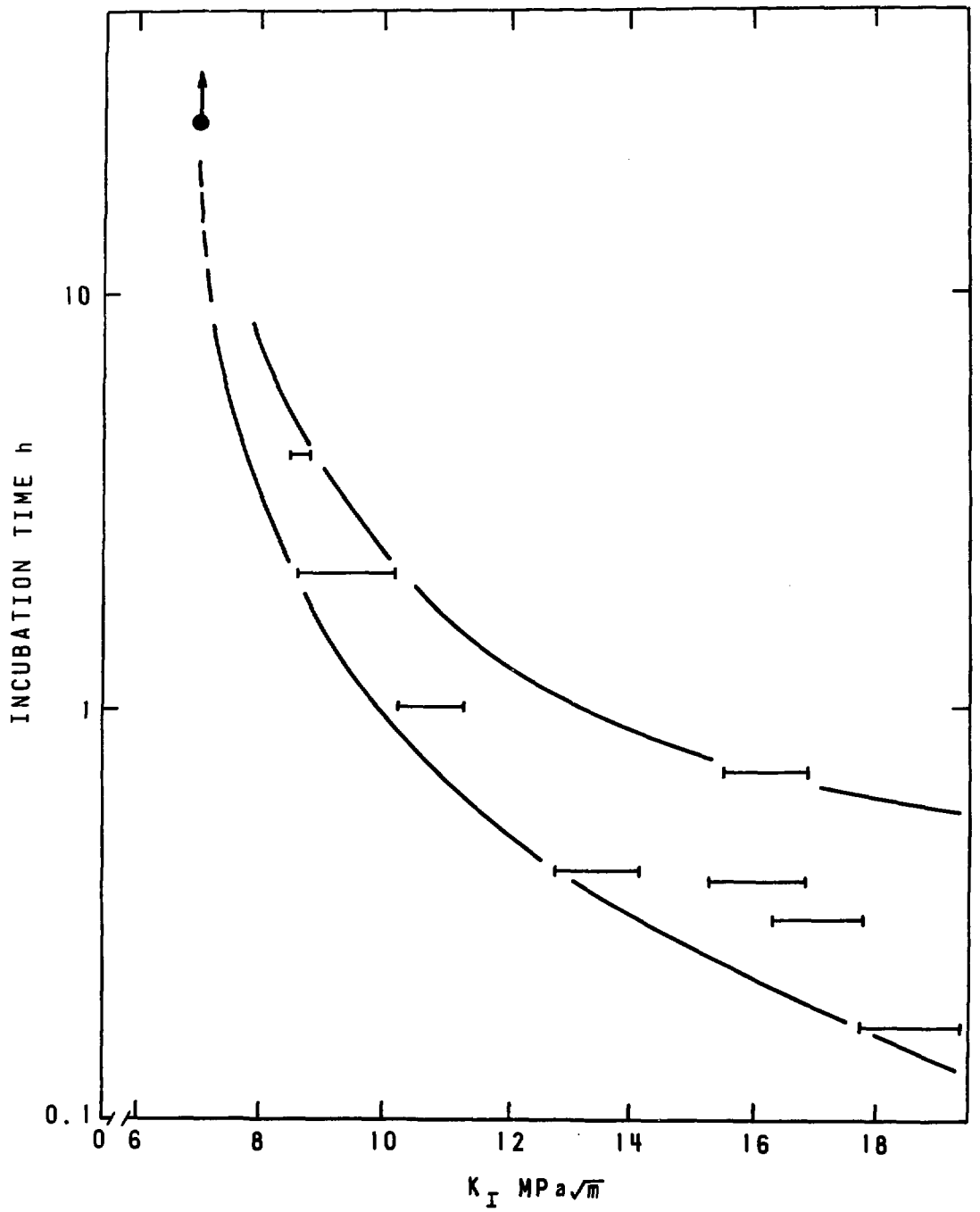

Figure 9: Dependence of crack incubation time on K_I for cantilever beam specimen of Zr-2.5 at% Nb tested at 500 K. Note the approach to K_{IH}.

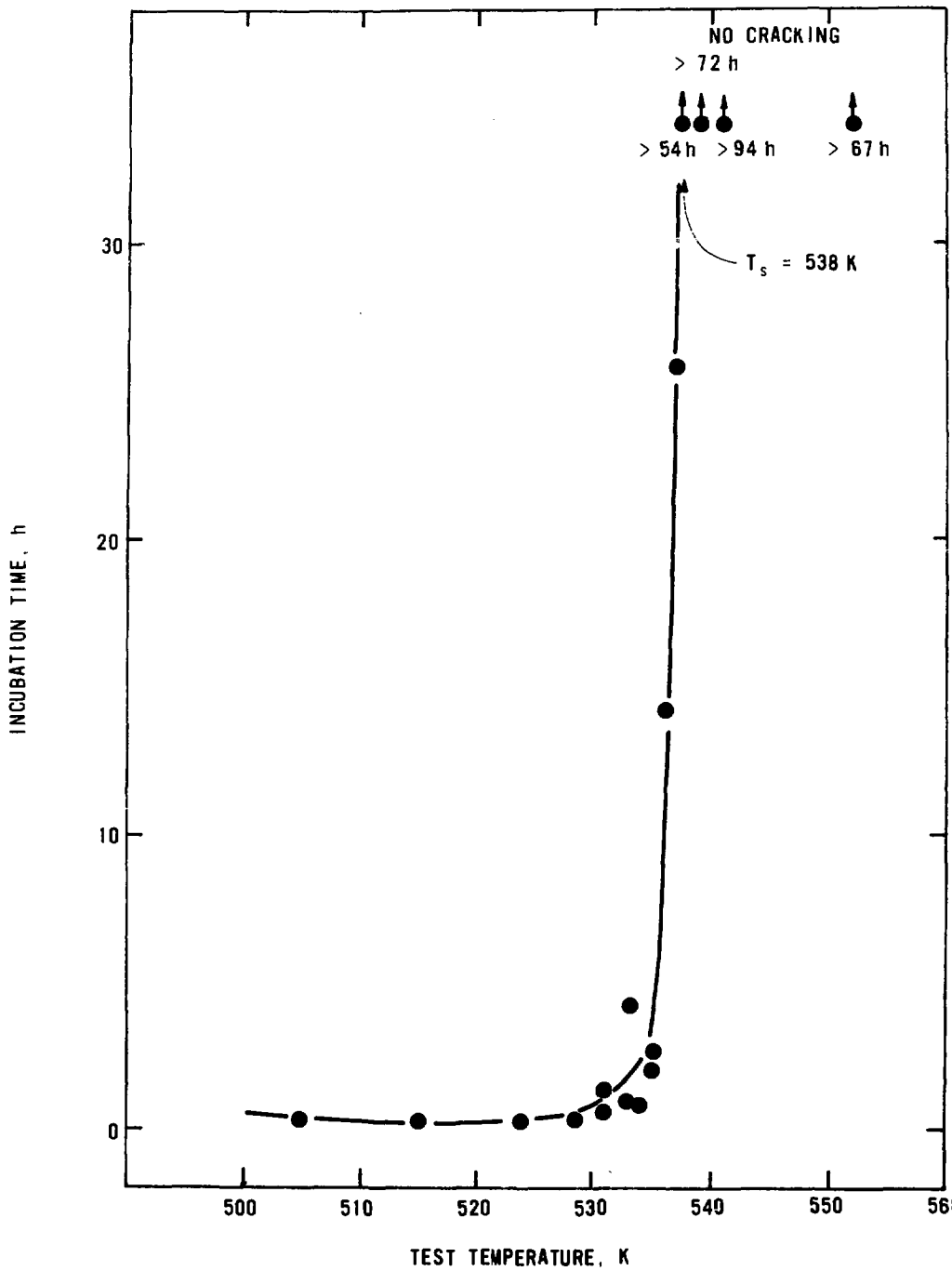

Figure 10: Temperature dependence of crack incubation time in cantilever beam specimen of Zr-2.5 at% Nb containing 0.13 at% protium and 0.29 at% deuterium. Note sudden increase in incubation time corresponding to solvus temperature of 538 K.

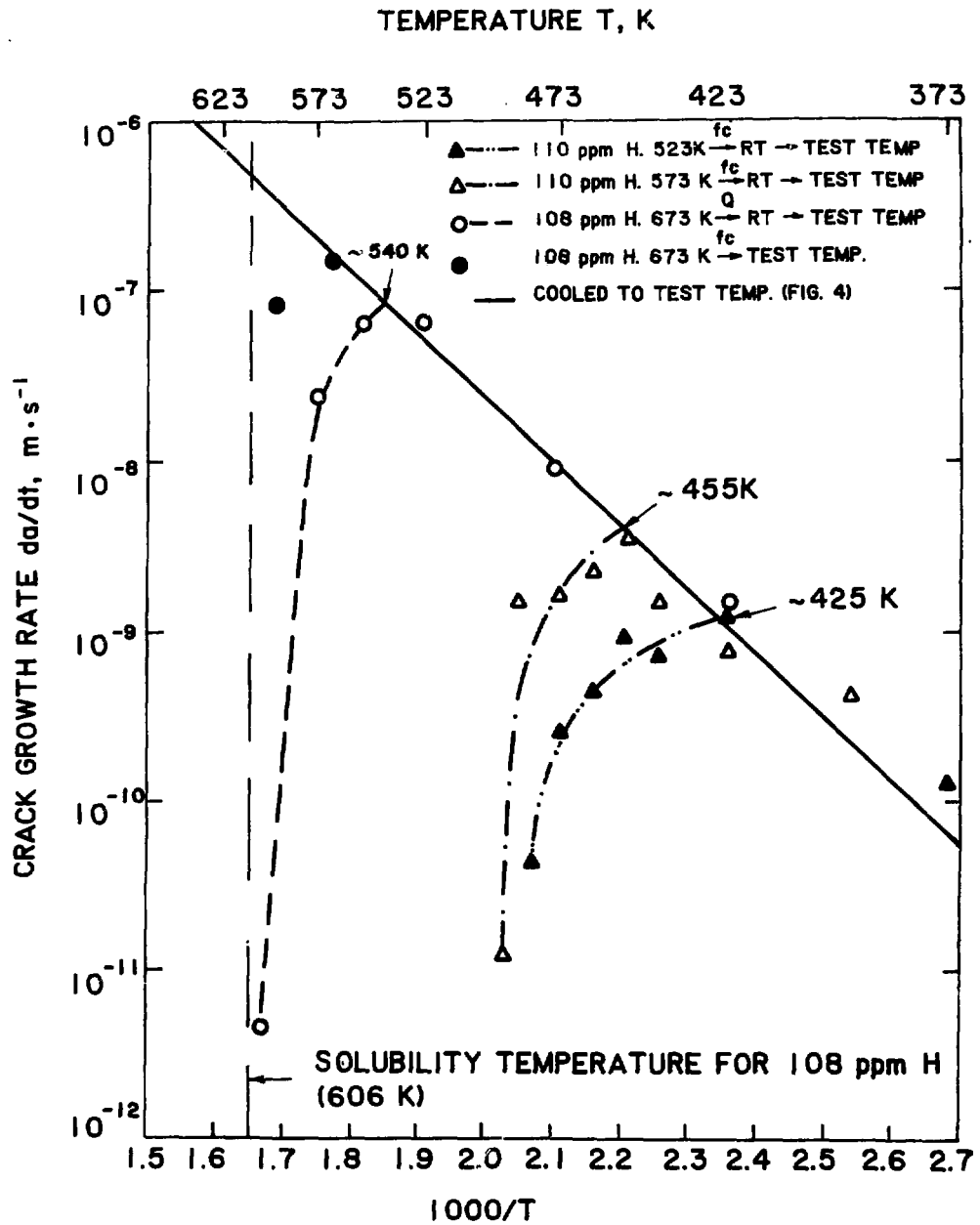

Figure 11: Temperature dependence of crack growth rate (as measured by acoustic emission) for Zr-2.5 at% Nb specimens after various heat-treatments and heated to the test temperature. Specimens contained 0.98 at% hydrogen.

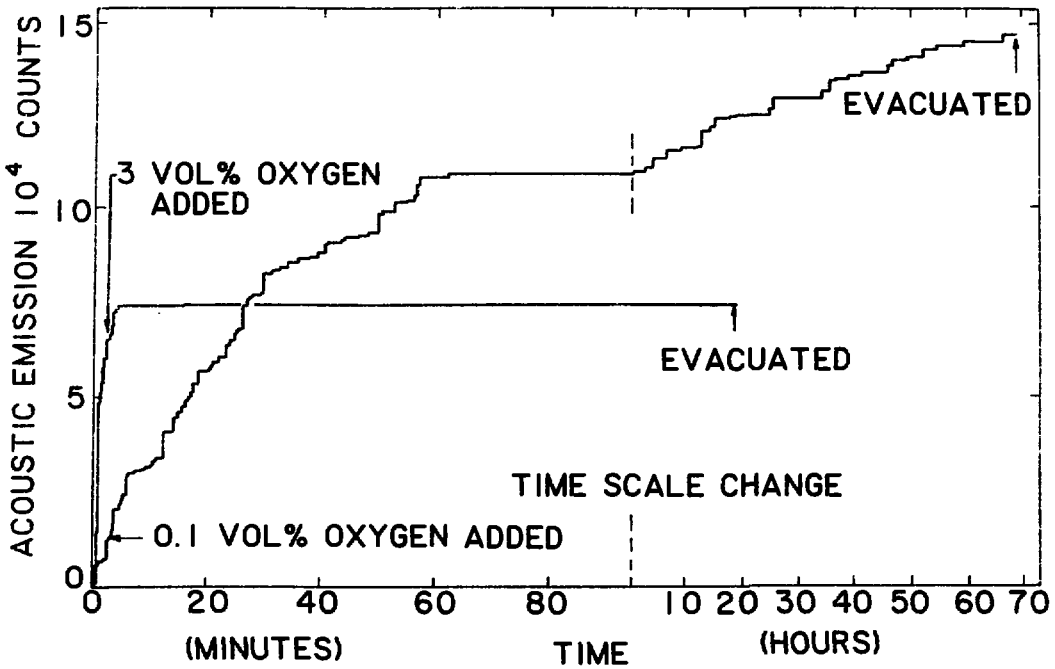

Figure 12: Suppression of cracking in Zr-2.5 at% Nb in a hydrogen atmosphere by small additions of oxygen.

ISSN 0067 - 0367

To identify individual documents in the series we have assigned an AECL- number to each.

Please refer to the AECL- number when requesting additional copies of this document

from

Scientific Document Distribution Office
Atomic Energy of Canada Limited
Chalk River, Ontario, Canada
K0J 1J0

Price: $2.00 per copy

ISSN 0067 - 0367

Pour identifier les rapports individuels faisant partie de cette série nous avons assigné un numéro AECL- à chacun.

Veuillez faire mention du numéro AECL- si vous demandez d'autres exemplaires de ce rapport

au

Service de Distribution des Documents Officiels
L'Energie Atomique du Canada Limitée
Chalk River, Ontario, Canada
K0J 1J0

Prix: $2.00 per copy

3548-86